Involvement of endoplasmic reticulum stress in β-cell apoptosis: a proteomic approach in INS-1E cells.

D'Hertog W.[1], Maris M.[1], Ferreira G.B.[1], Lage K.[2], Hansen D.A.[2], Cardozo A.K.[3],Workman C.T.[2], Moreau Y.[4], Eizirik D.L.[3], Waelkens E.[5,6] , Overbergh L.[1] and Mathieu C.[1].

Affiliations:

[1] Laboratory for Experimental Medicine and Endocrinology (LEGENDO), University Hospital Gasthuisberg, Catholic University of Leuven, Herestraat 49, box 902, B-3000 Leuven, Belgium

[2] Centre for Biological Sequence Analysis, BioCentrum-DTU, Technical University of Denmark, Building 208, DK-2800 Lyngby, Denmark

[3] Laboratory for Experimental Medicine, Université Libre de Bruxelles (U.L.B.), route de Lennik 808, box CP618, B-1070 Brussel, Belgium

4 *j*ESAT-SDC, Department of Electrical Engineering, Catholic University of Leuven, Kasteelpark Arenberg 10, box 2446, B-3001 Heverlee, Belgium

[5] ProMeta, University Hospital Gasthuisberg, Catholic University of Leuven, Herestraat 49, box 901, B-3000 Leuven, Belgium

[6] Laboratory of Biochemistry, University Hospital Gasthuisberg, Catholic University of Leuven, Herestraat 49, box 901, B-3000 Leuven, Belgium

Corresponding author:

Lut Overbergh, PhD, LEGENDO, UZ-Gasthuisberg, Onderwijs en Navorsing, Herestraat 49, bus 902, B-3000 Leuven, Belgium. E-mail lut.overbergh@med.kuleuven.be; Tel: 00-32-16-34.61.63; Fax: 00-32-16-34.60.35

Running title:

Involvement of endoplasmic reticulum stress in β-cell apoptosis

Abbreviations:

ATF6: activating transcription factor 6

CHOP: CCAAT/enhancer binding protein

CPA: cyclopiazonic acid

EF2: elongation factor 2

ER: endoplasmic reticulum

hnRPK: heterogeneous nuclear ribonucleoprotein K

HPRT: hypoxanthine-guanine phosphoribosyltransferase

HSPA5: 78 kDa glucose-regulated protein

HSPA8: heat shock 70 kDa protein 8

HYOU1: hypoxia up-regulated protein 1

IFN-γ: interferon gamma

IL-1β: interleukin-1 beta

IRE1a: inositol-requiring ER-to-nucleus signal kinase 1 a

PCSK2: prohormone convertase 2

PDIA6: protein disulfide-isomerase A6

PERK: protein kinase RNA-dependent-like ER kinase

UPR: unfolded protein response

Summary

Exposure of insulin secreting β-cells to inflammatory cytokines or nutrients, factors involved in the pathogenesis of type 1 and type 2 diabetes, leads to endoplasmic reticulum (ER) stress, β-cell dysfunction and eventually apoptotic β-cell death. RNA studies suggest that ER stress is a major contributor to β-cell dysfunction and death. The aim of this study was to analyze the protein changes induced by ER stress, in order to gain insight on the exact role of ER stress in β-cell damage. For this purpose, we have exposed insulin-producing rat INS-1E cells *in vitro* to the reversible ER stress inducer cyclopiazonic acid (CPA) at two different concentrations (6.25µM and 25µM), representing low and high ER stress levels. Protein changes were evaluated using 2D-DIGE, followed by MALDI-TOF/TOF at three different time points (6h, 12h and 24h). In INS-1E cells, 25µM CPA led to massive apoptosis, accompanied by a near complete protein translation shut-down, indicating a higher sensitivity of INS-1E cells to CPA-induced ER stress compared to other endocrine cells (rat adrenal medulla derived PC12). The lower concentration of CPA (6.25µM) led to adaptation of ER stress. Identification of the differential expressed proteins in the two conditions identified a clear pattern of defense pathways, with posttranslational modifications playing a crucial role. Moreover, many discrepancies with RNA findings were observed, suggesting that this latter technique may not be optimal for analyzing effects of ER stress, as many effects will only appear posttranscriptionally. We conclude that insulin secreting INS-1E cells are excessively sensitive to pure ER stress and that studying posttranscriptional and posttranslational modifications are of major importance to understand the impact of ER stress on β-cell function and survival.

Introduction

Pancreatic β-cells are responsible for synthesizing, processing and secreting the peptide hormone insulin into the circulation, thus maintaining normal blood glucose levels, a situation which is imbalanced in both type 1 and type 2 diabetic patients. Because of this metabolic role focused on insulin processing, β-cells have a highly developed endoplasmic reticulum (ER). Proper function of the ER is essential for β-cell survival and perturbation of its function induces cellular damage, eventually resulting in apoptosis. Various conditions, like inhibition of protein glycosylation, impaired formation of disulfide bonds and calcium depletion from the ER lumen can disturb ER function. Accumulation of unfolded or misfolded proteins in the organelle is met by a self-protective mechanism against ER stress, the unfolded protein response (UPR). This is mediated through the action of three pathways, namely protein kinase RNA-dependent-like ER kinase (PERK), activating transcription factor 6 (ATF6) and inositol-requiring ER-to-nucleus signal kinase 1 a (IRE1a). The UPR is a protective pathway which decreases ER protein levels and restores ER function by different mechanisms, such as 1) attenuation of protein translation through activation of the PERK – eukaryotic translation initiation factor 2alpha (eIF2alpha pathway); 2) up-regulation of ER chaperones through activation of the ATF6 – X-box binding protein 1 (XBP1) pathway; 3) degradation of misfolded proteins through activation of the ER degradation pathway (ERAD); and 4) halting new protein production via activation of IRE1 (1, 2). In case of prolonged or excessive ER stress, the different steps activated by the UPR response fail to restore ER homeostasis and apoptotic pathways are triggered.

Cyclopiazonic acid (CPA) is produced by *Penicillium cyclopium* as a secondary metabolite and is a highly selective and reversible inhibitor of the sarco-endoplasmic reticulum pump (SERCA-pump), thereby depleting the ER from Ca^{2+}. CPA is thus used as a well established model for the induction of pure ER stress. Also cytokines are known to cause ER stress, at least in part, through inhibition of the same SERCA pump, via activation of iNOS and nitric oxide production (3) and JNK activation (4), as well as through activation of inositol 1,4,5-trisphosphate receptor type 2 (IPTR2) (5), both

leading to a depletion of intracellular Ca^{2+} stores. We choose the well established rat cell line INS-1E (6), which is considered an accepted *in vivo* model for the study of β-cells. Taking into account the high amount of cells necessary for proteomic analysis, using a cell line opens the possibility to investigate different experimental conditions, i.e. different time points combined with different concentrations of CPA. In the present study we now investigate the global changes induced by CPA at the protein level.

The results point to two different mechanisms. INS-1E cells under high ER stress quickly and massively go in apoptosis. We observe major defects in insulin processing, suggesting that not only insulin mRNA expression is decreased upon ER stress, but also the conversion of pro-insulin to insulin. Also, marked decreases in different ER chaperones are observed, a phenomenon that is not observed at mRNA level. This indicates that important differences at mRNA and protein or even post-translational level are taking place in the process of ER-stress mediated β-cell death. As these INS-1E cells are extremely sensitive to ER stress as compared to other secretory cell types like e.g. the rat pheochromocytoma cell line PC12, we want to assess the effect of a lower dose of CPA (6.25μM) as a model for low ER stress, where the molecular mechanisms behind ER stress might be more visible. Under low ER stress, the INS-1E cells are able to adapt, as deducted at the protein level by the transient downregulation or inactivation of many proteins involved in cell fate, followed at later time points by upregulation or activation.

Experimental procedures

Cell culture conditions

INS-1E cells, a kind gift from Prof. C. Wollheim (Centre Medical Universitaire, Geneva, Switzerland), were cultured in RPMI 1640 (Cambrex, Belgium) supplemented with 10 mmol/l HEPES, 10% v/v heat-inactivated fetal calf serum, 100 units/ml penicillin, 100 µg/ml streptomycin, 1 mmol/l sodium pyruvate, and 50 µmol/l β-mercaptoethanol. Cells used for experiments ranged from passage 62 until 66 (6). The presently used INS-1E cells have a well-preserved insulin release in response to glucose (6) and respond to cytokines and CPA in a similar way as primary β-cells (7). PC-12 cells were cultured in F-12K Nutrient Mixture Kaighn's modification medium supplemented with 15% horse serum, 2.5% fetal bovine serum, 100 units/ml penicillin, and 100 g/ml streptomycin. Cells or whole islets from rat (isolation see below) were treated with CPA (Sigma, Bornem, Belgium) dissolved in DMSO and used at a final concentration of 3.1µM; 6.25µM; 12.5µM or 25µM. Control cells were treated with DMSO alone. For cytokine treatment 10 units/ml recombinant human IL-1β (a kind gift from Dr. C. W. Reinolds, National Cancer Institute, National Institutes of Health, Bethesda, MD) and 500 units/ml recombinant rat IFN-γ (R&D Systems, Minneapolis, MN) were used.

Rat islet isolation

Wistar rats were purchased from xxx. Islets from young rats (1 week of age) were isolated as described previously (8).

Cell death analysis

For the INS-1E cells, the percentage of living, apoptotic and necrotic cells was assessed by cell counting. INS-1E cells were cultured in 96-well plates (8000 cells/well). After 6, 12h and 24h of exposure cells were incubated for 15 min with propidium iodide (10 µg/ml)(Invitrogen, Merelbeke, Belgium) and Hoechst HO 342 (20 µg/ml)(Invitrogen,

Merelbeke, Belgium). A minimum of 500 cells was counted in each experimental condition by two researchers, one of them unaware of the sample identity, on an inverted fluorescent Ti-E microscope (Nikon, Brussels, Belgium).

For the rat islets, the percentage of living and death cells was assessed by cell counting. Wistar rat islets were cultured in 96-well plates (15 to 20 islets /well). After 24h of exposure to 25µM CPA or control condition, islets were incubated for 15 min with propidium iodide (10 µg/ml) and Hoechst HO 342 (20 µg/ml). Rat islets were counted in each experimental condition by two researchers, one of them unaware of the sample identity, on an inverted fluorescent Ti-E microscope (Nikon, Brussels, Belgium).

Real-time RT-PCR

Total RNA was extracted from 5 x 10^5 cells using the High Pure RNA Isolation Kit (Roche, Vilvoorde, Belgium) and 0.5µg was reverse transcribed using 100U Superscript II RT (Life Technologies, Merelbeke, Belgium) at 42°C for 80min, in the presence of 5µM oligodT_{16}. Real time PCR was performed for CHOP10, HSPA5, HYOU1, PDIA6 and HPRT using TaqGold (Eurogentec, Belgium), TaqMan probes or Syber-Green, and the MyiQ system (Bio-Rad, Nazareth, Belgium) as described previously (9). The following primers were designed making use of the software program Primer3 (10): CHOP10-FW: 5'-TCTCATCCCCAGGAAACGAA-3'; CHOP-RV: 5'-ATCTGGAGA-GCGAGGGCTTT-3'; and CHOP-TP: 5'-ACCCTGCGTCCCTAGCTTGGCTG-3'. INS2-FW: 5'- GCTGGCCCTGCTCATCCT-3'. INS2-RV: 5'-CCACCAAGTGAGAACCACAAAG-3'. HPRT-FW: 5'-TTATCAGACT-GAAGAGCTACTGTAATGATC-3'; HPRT-RV: 5'-TTA-CCAGTGTCAATTATATCTTCAACAATC-3'; and HPRT-TP 5'-TGAGAGATCATC-TCCACCAATAACTTTTATGTCCC-3'. HYOU1-FW: 5'-CACATGGCACAGATTG-AAGG-3'; and HYOU1-RV: 5'-CAGGCACTCGATCAAACAAA-3'. PDIA6-FW: 5'-GCAGCAAGTGCACTGAAAGA-3'; and PDIA6-RV: 5'-GGAAATCCCTGGACAC-CATAC-3'. HSPA5-FW: 5'-ACCTATTCCTGCGTCGGTGT-3'; HSPA5-RV: 5'-AGGAGTGAAGGCCACATACGA-3' and HSPA5-TP: 5'-

AAGAACGGCCGCGTGGAGATCAT-3'. Normalization was performed using the housekeeping gene hypoxanthine-guanine phosphoribosyltransferase (HPRT), for which no regulation by the treatment itself was observed. Quantification was based on the ΔΔCt method. Where necessary, a correction for differences in efficiency between target and housekeeping gene was performed using the Pfaffl method (11).

2D-DIGE analysis

$8.5x10^6$ INS-1E cells were incubated during 6, 12 or 24h with 6.25µM CPA or, with 25µM CPA during 6 or 12h. Control cells were treated with DMSO alone. Quadruplicate experiments were performed, originating from 4 independent experiments. Sample collection and processing was performed as described earlier (5). Protein samples were separated in the first dimension using two pH ranges (pH4-7 and pH6-9) on 24cm strips (GE Healthcare, Diegem, Belgium). First and second dimension were performed as described earlier (5).

Spot digestion and protein identification by MALDI-TOF/TOF analysis

For spot picking, two preparative gels for each pH range were run (350µg protein lysate each). First and second dimension runs were performed as described (5), except that Cy Dye-labeling was omitted. Glass plates were pre-treated with BindSilane and two reference markers were applied to enable automatic picking. The gels were post-stained using Krypton (Pierce, Rockford, USA). Matching with the analytical gels was performed using the BVA module of the DeCyder V6.5 software. A pick list was generated and exported into the Spot Picker V1.20 software which controls the Ettan Spot Picker (GE Healthcare).

Spot digestion and peptide purification was performed as previously reported (5).

MS/MS analyses were performed on a 4800 MALDI TOF/TOF (Applied Biosystems, CA, USA). The instrument was calibrated with the Applied Biosystems Calibration Mixture 1. Measurements were taken in the positive ion mode between 900 and 3000 m/z. Sequences were automatically acquired by scanning first in MS mode and selecting the 15 most intense ions for MS/MS using an exclusion list of peaks arising from tryptic auto-digestion. Air was used as the collision gas, while the collision energy was adapted automatically. Data interpretation was carried out using the GPS Explorer software (V3.6) and database searching was carried out using the Mascot program (version 2.2.00). Since all experiments were performed on rat INS-1E cells, MS/MS searches were conducted in the following databases with the taxonomy set on *Rattus*: NCBI (3446 sequences), MSDB (20748 sequences) and SwissProt (5769 sequences). MS/MS tolerance for precursor and fragment ions was set between 0.2 Da and 1 Da depending on the sample, methionine oxidation as variable modification and carbamidomethylation of cysteine as fixed modification. As enzyme, trypsin was selected and a maximum of one missed cleavage was allowed. Using these parameters the probability-based MOWSE scores greater than the given cut-off value for MS/MS fragmentation data were taken as significant ($p<0.05$).

Interactome network analysis

Network analysis was performed as reported in previous work (5) based on (12, 13).

Western blotting

$2.5x10^6$ INS-1E cells were cultured as described above. The cells were lysed in 150mM NaCl, 1mM $CaCl_2$, 1mM $MgCl_2$, 10mM NaF, 1% NP-40, 1mM Na_3VO_4, 1mM phenylmethylsulfonyl fluoride and a protease inhibitor cocktail (Complete Protease Inhibitor, Roche Diagnostics, Basel, Switzerland). Protein concentrations were determined using the BCA Protein Assay Reagent Kit (Perbio Science, Aalst, Belgium). 10µg cell lysate was denatured using NuPage Sample Buffer (4X), NuPage 10X

Reducing Agent and heated for 10min at 70°C, before loading on a 4-12% NuPage Bis-Tris gel. Proteins were transferred to an Amersham Hybond LFP Low-fluorescent PVDF membrane (GE Healthcare). Protein electrophoresis and electroblotting were performed following the instructions of the manufacturer. Equal loading and transfer efficiency was tested by staining for β-actin. Previously blocked membranes were incubated overnight at 4°C with one of the following antibodies: anti-CHOP (1/350, Santa Cruz Biotechnology, Santa Cruz, USA), anti-actin (1/12000, Sigma, Bornem, Belgium), anti-HYOU1 (1/5000, Abcam, Cambridge, UK), anti-HSPA5 (1/500, Santa Cruz Biotechnology, Santa Cruz, USA), anti-PDIA6 (1/5000, Abcam, Cambridge, UK). Imaging and quantification of the blots was done using the ECL-plex (GE Healthcare) goat-anti-mouse Cy2 and goat-anti-rabbit Cy5 secondary antibodies and subsequent scanning of the blots on the Typhoon scanner. Image analysis and quantification of the bands was performed using ImageQuant TL (v2003).

ELISA

Insulin release was measured upon stimulation with low (3mM) or high (20mM) glucose concentration. After incubation, INS-1E cells were washed twice with pre-warmed glucose-free Krebs-Ringer HEPES bicarbonate (KRHB) (134mM NaCl, 4.7mM KCl, 1.2mM $NaH_2PO_4.H_2O$, 1.2mM $MgSO_4.7H_2O$, 1mM $CaCl_2.2H_2O$, 5mM $NaHCO_3$, 10mM HEPES, 0.5% BSA) and equilibrated for 30min at room temperature. The solution was replaced with KRHB with either 3mM or 20mM glucose and incubated for 1h at 37°C. Insulin content in the supernatant was determined using the rat insulin ELISA kit from Mercodia (Uppsala, Sweden), according to the manufacturer's guidelines.

Statistical analysis

For 2D-DIGE experiments the one-way ANOVA and the paired Student's t-test was used. To analyze differences in protein levels, the Decyder V6.5 software was used, and a p-value of less than or equal to 0.05 was considered statistically significant. For all other

tests the paired Student’s t-test was used and $p<0.05$ was considered statistically significant.

Results

Effect of CPA on apoptosis susceptibility of INS-1E cells, compared to whole islets and PC12 cells.

To investigate the susceptibility of INS-1E cells to CPA-induced apoptosis, cells were cultured for 6h, 12h or 24h in the presence of different concentrations of CPA, ranging from 3.1µM to 25µM. For the lowest concentration of 3.1µM CPA, no apoptosis was induced at any of the time points investigated. When using higher concentrations of 6.25µM and 12.5µM CPA, the percentage of apoptotic cells increased in a dose dependent manner. Using the highest concentration of 25µM CPA, the proportion of apoptotic cells increased from 2.8±1.1% in control condition to 10.3±1.7% ($p<0.05$) after 6h of exposure, increasing to 22.9±0.9% ($p<0.001$) after 12h, resulting in a massive induction of apoptosis after 24h treatment (39.8±4.5% apoptotic cells versus 1.9±1.0% in control condition, $p<0.001$) (Fig. 1a). No significant increases in the level of necrosis were observed in any of the conditions analyzed (data not shown).

This increase in apoptosis was paralleled by a massive increase in transcript levels for the pro-apoptotic transcription factor CHOP. No increase in CHOP mRNA levels was observed using 3.1 or 6.25µM CPA. Using the higher concentrations of 12.5 or 25µM, a marked induction of CHOP mRNA levels was observed, and this already from 6h onwards (17.5-, 4.8-, and 3.5-fold for 12.5µM and 49.8-, 28.1- and 23.1-fold for 25µM; $p<0.05$ compared to control for all conditions) (Fig. 1b). This was paralleled by an increase in CHOP protein levels, as measured upon 25µM CPA stimulation (8.8-fold after 6h ($p<0.05$, $n=3$) and 7.3 fold after 12h ($p<0.01$, $n=3$) (Fig. 2) (14). These findings are in agreement with our previous findings, confirming that CPA specifically induces apoptosis, and not necrosis, in INS-1E cells.

The susceptibility of INS-1E cells was compared to CPA-induced apoptosis in whole rat islets. Here, using 25µM CPA, an increase in apoptosis was observed after 24h (from

17.8±1.4% apoptosis in control to 36.4±1.3% apoptosis in islets treated with CPA, p<0;001, n=3).

The susceptibility of INS-1E cells was compared to CPA-induced apoptosis in PC12 cells. Here, using the same concentration of CPA (25µM), only a minor increase in apoptosis after 24h was induced (2.7±2.1% to 7.4±3.1%, p<0.05). This was indicative for a higher susceptibility of INS-1E cells to ER-stress induced apoptosis as compared to PC12 cells.

Effects of high concentrations of CPA (25µM) on INS-1E cells

Alterations in proteomic profile: 2D-DIGE analysis.

Differential proteomic profiles of INS-1E cells were determined after exposure to 25µM CPA, and this after 6h and 12h of exposure. Quadruplicate experiments were performed for each of these time points, comparing CPA-treated with control INS-1E cells (Suppl. Fig. 1). Within two different pH ranges (4-7 and 6-9) a total of 2729 ± 47 matched spots were detected. Of these, 44 and 90 spots were differentially expressed after 6h and 12h of CPA exposure, respectively. These originated exclusively from the pH4-7 range, as no differentially expressed spots were observed in the pH6-9 range. We were able to unambiguously identify 31 (70.5%) and 43 (47.8%) spots at 6h and 12h, respectively. This resulted in a total of 47 different proteins, due to the presence of post-translationally modified forms in 9 of the identified proteins.

According to their sub-cellular localization, most of the identified proteins resided in the cytosol (36%), the nucleus (17%) and in the ER (15%), indicating that besides the expected relatively high amount of alterations observed in the ER, also important secondary effects outside the ER were picked up. According to their function, the identified proteins and their isoforms were classified into the following groups: 1) metabolism (18 proteins), 2) protein synthesis, modification, secretion or degradation (18 proteins), 3) processing of peptides and neurotransmitters (6 proteins), 4) cell adhesion, cytoskeleton and related genes (5 proteins), 5) RNA synthesis/turnover (10 proteins), 6)

cell cycle and related genes (5 proteins), 7) defense/repair (1 protein), 8) calcium binding (3 proteins) and 9) miscellaneous (3 proteins).

Interestingly, some crucial proteins involved in insulin processing were clearly down-regulated, namely prohormone convertase 2 (in 4 out of the 5 different isoforms identified) and thioredoxin domain containing protein 5 precursor (TXND5), an ER residing protein responsible for the formation of disulfide bonds (15). Also hnRPK, an RNA binding protein, was substantially downregulated in the 6 different isoforms identified, again most prominent at the early 6h time point.

A second group of proteins that was clearly altered in expression were molecular chaperones, involved in the folding and clearing the ER from misfolded proteins. Indeed, a marked decrease in expression was observed for the hypoxia up-regulated protein 1 (HYOU1), BiP (HSPA5), heath shock 70 kDa protein 8 (HSPA8) and protein disulfide isomerase A3 (PDIA3). Of note, 5 different isoforms were detected for HYOU1, all of them being downregulated at 6h. For HSPA8, on the other hand, an up-regulation of one isoform opposed to a down-regulation of a second isoform, suggested an effect of CPA specifically on the modification, possibly by de-phosphorylation. For HSPA5, a significant downregulation was observed only in the third major isoforms of the protein at 6h (the two times modified isoform). However, all three major isoforms showed the same tendency to be downregulated at 6h and 12h. The combined downregulation of these different chaperones pointed towards a defective response and the inability of the cell to cope with the high amount of ER stress.

Interactome-network

From the 19 unique proteins identified at 6h, 17 were found to be in an interaction network ($p<1e-6$) (Suppl Fig. 2A). hnRPK and HSPA5 were centrally located in this network, thus confirming their crucial role in altering the proteome profile at this early 6h time point. At 12h the picture is less clear, with only 24 out of the 42 unique proteins represented in an interaction network ($p<1e-6$) (Suppl Fig. 2B). This may point towards a deterioration of the cellular state of the INS-1E cells upon treatment with 25µM CPA,

consistent with the finding that the majority of the protective proteins were downregulated and a massive induction of apoptosis was seen.

Alterations in chaperone levels: western blotting and quantitative RT-PCR

In order to validate the data obtained from 2D-DIGE, as well as to compare with previously performed microarray data (16), western blot analysis and quantitative RT-PCR were performed for key chaperones abundantly expressed and clearly altered by CPA treatment. For this purpose, we chose to investigate levels of HYOU1, HSPA5 (altered in 2D-DIGE and induced in expression in microarray (16)) and PDIA6 (only induced in microarray analysis).

At the mRNA level HSPA5 was significantly induced from 6h of incubation on (2.6-fold, $p<0.01$, n=3) and stayed upregulated at 12h and 24h (3.0-fold and 2.9-fold respectively, $p<0.01$, n=3). Similarly, HYOU1 mRNA was significantly induced from 6h of incubation on (1.5-fold, $p<0.05$, n=3) and stayed upregulated at 12h and 24h (2.0-fold and 2.3-fold, respectively, $p<0.01$, n=3). Finally, a similar regulation was observed for PDIA6, with mRNA levels increasing 1.3-, 1.3- and 1.6-fold after 6, 12 and 24h of CPA exposure, respectively ($p<0.05$ for 6 and 12h, n=3 and $p<0.01$ for 24h) (Fig. 3).

No significant alterations were observed in total protein levels, as analyzed by western blotting, for any of the 3 chaperones investigated (p=NS, n=3), and this after 6, 12 and 24h of CPA exposure, suggesting that post-transcriptional regulation is taking place. Moreover, the absence of regulation at the total protein level was, at least for HSPA5 and HYOU1, not consistent with the differential regulation observed in 2D-DIGE. Therefore, rather a shift in post-translational modification was taking place. This underscores the importance of gel-based proteomic studies, making the analysis of post-translational modified forms possible, as opposed to western blotting.

Treatment of PC12 cells with the same (25 µM) concentration of CPA resulted in an appropriate upregulation of the most important ER chaperone, HSPA5. mRNA levels were already increased after 6h of exposure (6.6 fold, $p<0.005$, n=3), and returned to

control levels after 24h. Also protein levels of HSPA5 were increased, with a 23 and 17-fold induction, after 12 and 24h, respectively.

Alterations in proteins involved in insulin processing: functional implications

One of the major effects of pronounced concentrations of CPA on INS-1E cells was on proteins involved in insulin processing, such as prohormone convertase 2. In line with this, also a marked down-regulation in PCSK2 mRNA levels was observed (36% and 40% of control at 12 and 24h, respectively ($p<0.01$, $n=3$)). In parallel, also insulin 2 mRNA levels were significantly decreased, to 30%, 12% and 16% of control levels after 6, 12 and 24h, respectively ($p<0.01$, $n=3$) (Fig. 4).

Based on the alterations observed in proteins involved in insulin processing, we further evaluated if these changes led to a functional impairment in insulin release. As anticipated, 25µM of CPA significantly reduced glucose-induced insulin release in INS-1E cells at 6, 12 and 24h upon stimulation with 20mM glucose (58%, 64% and 72% reduction, respectively ($p<0.01$, $n=3$)) (Fig. 5).

Effects of low concentrations of CPA (6.25µM) on INS-1E cells

Alterations in proteomic profile: 2D-DIGE analysis.

In analogy to the exposure of INS-1E to high concentrations of CPA, a quadruplicate proteomic analysis was performed after exposure to 6.25µM CPA, and this at different time points (6, 12 and 24h of exposure). Opposed to the minor effects on apoptosis induction, this lower concentration of CPA exposure had great impact on the proteomic profile. 131, 48 and 86 spots were differential expressed at 6, 12 and 24h, respectively. Of these, 101 (77.1%), 34 (70.8%) and 55 (64.0%) were identified. According to their function, the identified proteins and their isoforms were classified into the following groups: 1) metabolism (73 proteins), 2) protein synthesis, modification, secretion or degradation (45 proteins), 3) processing of peptides and neurotransmitters (8 proteins), 4) cell adhesion, cytoskeleton and related genes (22 proteins), 5) RNA synthesis/turnover (20 proteins), 6) cell cycle and related genes (4 proteins), 7) defense/repair (4 protein), 8)

calcium binding (2 proteins) and 9) miscellaneous (16 proteins). (Suppl. Table 1). Remarkably, the proportion of altered metabolic proteins was much more pronounced as compared to the 25µM CPA exposure (37% versus 27%). Sub-cellular localization for these identified proteins revealed a majority of cytoplasmic protein (41.3%), while true ER proteins were found to account only for 8.4%.

Exposure of INS-1E cells to 6.25µM had great impact on the metabolic proteins of the cell. Out of the 32 unique metabolic proteins identified at 6h, 18 were related to the Krebs cycle or glycolysis. The majority of these were transiently downregulated at 6h, where after their level normalized (Fig. 6). A second transient effect was observed on the regulation of elongation factor 2 (EF2). After 6h of exposure, 5 different isoforms of EF2 significantly decreased (ranging from 1.16 till 1.78-fold). This down-regulation was aborted at 12 and 24h, with two different isoforms being slightly upregulated (1.14 and 1.17 times), pointing to a transient attenuation of protein translation upon low levels of ER stress.

As for the high 25µM CPA concentration, clear effects of 6.25µM CPA were observed on proteins involved in insulin processing. Again different isoforms of PCSK2 were markedly downregulated and this in several different isoforms. This was evident already at the early 6h time point and remained till 24h of stimulation. Also notable in this regard was the marked increase in chromogranin A, B and C (CGA, CGB and SCG2) after 24h of exposure to 6.25 µM CPA, which was much more pronounced then after high-dose CPA exposure. The observed upregulation of CGA and CGB combined with the observed decrease in PCSK2 levels pointed towards a defective insulin processing and release by the INS-1E cell upon mild ER stress. Also several isoforms of hnRPK, as well as another RNA binding protein, namely hnRP A1, were clearly downregulated.

Again significant alterations were observed in different ER chaperones, namely HSPA5, HYOU1, PDIA6, ERP29, HSP60, HSPA8 and HSP74. Interestingly, the picture for HSPA5 showed a down-regulation of the unmodified form, accompanied by an increase

of different modified isoforms after 6h of exposure. This was a transient regulation, since levels were opposite after 24h of exposure.

Interactome-network analysis of altered proteins by CPA

From the 87, 34 and 41 unique proteins identified at 6, 12 and 24h; 60, 13 and 32 respectively, were found to be in an interaction network ($p<5e-6$ for all) (Suppl. Fig. 2). Both the networks obtained after 6h and 24h of exposure showed a very tight interaction with the majority of altered proteins, while after 12h of exposure the network contained much less proteins. This reflected the finding that 12h was a time point in which many of the proteins were transiently normalized before going to an opposite regulation at 24h of exposure. The network obtained at 6h showed a central role for all the chaperones and RNA binding proteins, being connected to many proteins of other functional classes such as metabolic proteins and cytoskeleton proteins. Also of note was the marked up-regulation of two anti-apoptotic 14-3-3 proteins, the beta/alpha and the zeta/delta form, exclusively at the early 6h time-point. Since these 2 proteins were linked to an enormous number of other proteins in the network, they were also thought to play an active, central role in the ER stress process. At 24h, although the regulation of most of the chaperones was opposite as compared to 6h of exposure, they were still centrally located in the network, again suggesting a crucial role for the chaperones in the adaptation to ER stress.

Alterations in chaperone levels: confirmation by western blotting and quantitative RT-PCR.

To further strengthen the findings of the 2D-DIGE analysis, one of the essential ER chaperones, namely HSPA5, was analyzed by western blotting and real-time RT-PCR. Investigating total amounts of HSPA5 by western blotting, no regulation whatsoever was observed. In addition, only a minor effect on HSPA5 mRNA levels was observed, with a significant induction after 6h of CPA exposure ($p<0.01$, $n=3$) (Fig. 7). In the 2D-DIGE analysis however, we detected a shift in modification status of HSPA5, similar to previous results obtained with the cytokine-treated INS-1E cells (5). The major (first)

isoform of HSPA5 was downregulated (1.52 times at 6h ($p<0.05$)), while more acidic isoforms were upregulated at the same time point, indicative of inactivation. This pattern of regulation at the post-translational level was reversed at 24h, where the first (unmodified) isoform of HSPA5 was upregulated (2.56 times ($p<0.05$)) and the more acidic isoforms were downregulated.

Effects on insulin processing: Glucose stimulated insulin secretion

Because of the marked changes in proteins involved in insulin processing, we tested for this condition, as for the high-dose CPA (described above) if there was any functional impact on the glucose-regulated insulin release. A significant decrease of 44.5% in insulin release was observed, after 12h of low-dose CPA exposure ($p<0.05$) (Fig. 8).

Discussion

Endoplasmic reticulum stress has been put forward as a crucial mechanism involved in apoptotic β-cell death due to inflammatory cytokines or metabolic stressors like free fatty acids and glucose (5, 17-19). To gain more insight in the exact contribution of ER stress on this process, we have previously investigated the effects of a 'pure' ER stressor, namely cyclopiazonic acid (CPA) on INS-1E cells at the RNA level (16). As previously shown (5), major effects of ER stressors are also located posttranscriptionally and even more importantly posttranslationally. We extended the previous work by the present study, investigating global changes of ER stress at the protein level.

Our present results show that INS-1E cells, as well as rat β-cells cells, are excessively susceptible to pure ER stress. Relatively high levels of ER stress not toxic to other secretory cells provoked a massive induction of apoptotic cell death, accompanied by a decrease in insulin secretion, and a defective up-regulation of protective ER chaperones, such as HSPA5, not at the mRNA, but at the protein level. This discrepancy between RNA and protein levels points towards a compromised response. Indeed, PERK-eIF2a mediated translational attenuation, one of the classical UPR responses, does normally not include the mRNA encoding transcription factor ATF4 and its downstream genes, amongst which CHOP and HSPA5 (20). Of note, CHOP did respond normally to the stress situation by up-regulating its protein levels in follow-up of increased mRNA levels. Since an imbalance in the levels of HSPA5 versus CHOP is known to be crucial for the outcome of the cellular response (apoptosis versus adaptation) (21), the present findings may be one of the underlying mechanisms of the high susceptibility of INS-1E cells to apoptosis.

At very low concentrations of CPA, no apoptosis was induced and global alterations in protein profile indicate an adaptation of the cells to overcome the stress situation. Initially, multiple metabolic proteins were downregulated, pointing to a deterioration of the metabolic state of the cell. Functionally, this was accompanied by a decrease in glucose-stimulated insulin secretion. These findings were also observed at high CPA concentrations and were in line with previously performed microarray data (16), showing

a major decrease in insulin 1 and 2 mRNA levels, pointing towards a major effect of CPA on β-cell function. Interestingly, also cytokines had a major effect on the levels of PCSK2, an effect that was to a large extend caused by IL-1β, although exacerbated by addition of IFN-γ (5). This fits with the assumption that IL-1β mainly causes β-cell dysfunction and not β-cell death, most possibly through inhibition of the SERCA-pump and induction of ER stress. Another protein that was strikingly down-regulated was heterogeneous nuclear ribonucleoprotein K (hnRPK). This protein is involved in various processes, among which mRNA stabilization and translation, RNA splicing and chromatin remodeling (22, 23). hnRPK has a stabilizing function for the prepro-insulin mRNA through binding at the pyrimidin-rich 3' untranslated region (24, 25). The observed downregulation of hnRPK could thus have a further detrimental effect for the correct processing of insulin, here at the mRNA level. Related to this, another group of proteins that was markedly increased in expression were the chromogranins (CGA, SCG1 and SCG2). This was clear upon treatment with 25µM CPA, but even more pronounced with 6.25µM CPA. This appearance of chromogranins in their (high molecular weight) unprocessed isoform is possibly a direct consequence of the downregulation of PCSK2, the enzyme responsible for the processing of these proteins (26). The CGA-derived peptide pancreastatin has been reported to inhibit glucose-stimulated insulin release (27). Similar inhibitory functions have been shown for SCG1 (28) and possibly this latter protein takes part in the regulation of insulin secretion in the same way as CGA. The observed upregulation of CGA and SCG1 combined with the observed decrease in PCSK2 levels further supported a defective insulin processing and release by the INS-1E cell upon mild or severe ER stress.

Of interest, we observed that at a certain cross-point in time, the protein profile reversed and the cells survived even after long CPA exposure. The most striking example of this was HSPA5, for which total amounts of mRNA were slightly induced and total protein levels were not altered. However, an inactivation at the protein level at 6h was observed, due to a shift towards inactive post-translationally modified forms. At 24h the reverse was observed, resulting in activation of HSPA5. The exact nature of the post-translational modification is at present unknown, but would be consistent with either a

phosphorylation or ribosylation. Both these modifications have been described for HSPA5 upon glucose starvation and hypoxia (29, 30) and are thought to function as a rapid mechanism of reversible inactivation (31). Of note, a similar shift towards inactive post-translational modified forms of HSPA5 has also been reported upon cytokine stimulation of INS-1E cells (5), again suggesting an important contribution of ER stress in cytokine-induced β-cell death. A reversal of detrimental effects with 6.25µM CPA was also seen for proteins of other functional classes, such as many metabolic proteins, elongation factor 2 (EF2), and Bcl-2 inhibitor of transcription (PTRH2). These findings suggest an initial CPA-induced ER stress, which at a certain cross-point is driven towards adaptation/survival of the cells. Although the exact trigger resulting in reversal of the effects is not known, two centrally located proteins in the interactome network analysis, namely the 14-3-3 protein beta/alpha (YWHAB) and the 14-3-3 protein zeta/delta (YWHAZ)), are interesting candidates. 14-3-3 proteins play a role in regulation of diverse biological processes, among which survival/apoptotic signaling (32). They inhibit apoptosis through interaction with Bad complex formation resulting in inhibition of Bad:Bcl-X_L-mediated apoptosis (33-38), consequently promoting cell survival (39, 40). Proteins of the Bcl2 family, which are activated by the IRE1a--JNK- and IRE1a-CHOP pathway, play a major role in controlling cell-death upon ER stress triggered by Ca^{2+}-depletion, by modulating Ca^{2+} homeostasis (20). Moreover, another protein of this family, Bcl-2 inhibitor of transcription (PTRH2) was downregulated at the early 6h time point, while being induced after 24h, again promoting cell survival. The initial up-regulation of these two 14-3-3 family members at 6h upon low CPA stimulation could thus point to an inhibition of apoptosis by altering Bcl2 family members, leading to the observed survival of the cells.

Compared to previously performed proteomic analysis on cytokine-treated INS-1E cells, a similar defect in insulin signaling was observed as well as a similar post-translational regulation of HSPA5 (the latter only when compared to the low dose CPA), suggesting that cytokines at least in part act through induction of ER stress. A finding that is not surprising, since it is known that cytokines inhibit the SERCA pump, and induce the IPTR3 pump, thereby altering the Ca^{2+} concentration in the ER lumen. These findings are

in line with the recent findings of Wang et al, who demonstrated that IL-1β induced β-cell death is mediated in part by ER stress, also showing an important role of Ca^{2+} release through the JNK pathway (4). How to fit the data of Akerfeldt who at contrary showed an independency of ER stress on cytokine-induced β-cell death is not clear (41). Differences in cytokine and PBA (JNK inhibitor) concentration may possibly account for the different outcome on cell death.

In conclusion, these data prove the strong susceptibility of INS-1E cells, a model for β-cells, to pure ER stress, by executing an exaggerated effect on β-cell dysfunction and on the induction of apoptosis. At high levels of ER stress, the normal protective mechanisms, such as up-regulation of chaperones, are initiated at the mRNA level, but fail at the translational stage. At low levels of ER stress, survival is possible, although without restoration of β-cell function. Underlying processes involved in adaptation have been identified, with a possible crucial role for 14-3-3 proteins. A vital role for posttranslational modifications was observed, with a temporal inactivation of HSPA5 as the most striking example. The present study underscores the importance of proteomic analysis for gaining a better understanding on the impact of ER stress on β-cell function and survival.

Acknowledgments

This work was supported by the Catholic University of Leuven (GOA 2004/10 and 2009/10), the Flemish Research Foundation (FWO G.0552.06 G.0649.08), the Belgium Program on Interuniversity Poles of Attraction initiated by the Belgian State (IUAP P5/17 and P6/40) and the Centre of Excellence SymBioSys (Research Council K.U.Leuven EF/05/007). We gratefully acknowledge the technical assistance of Karin Schildermans, Sandy Vandoninck, Nursen Gol, Jos Depovere en Jos Laureys.

Reference List

1. Eizirik, D. L., Cardozo, A. K., and Cnop, M. (2008) The role for endoplasmic reticulum stress in diabetes mellitus. *Endocr. Rev.* 29, 42-61

2. Rutkowski, D. T., and Kaufman, R. J. (2004) A trip to the ER: coping with stress. *Trends Cell Biol.* 14, 20-28

3. Cardozo, A. K., Ortis, F., Storling, J., Feng, Y. M., Rasschaert, J., Tonnesen, M., Van Eylen, F., Mandrup-Poulsen, T., Herchuelz, A., and Eizirik, D. L. (2005) Cytokines downregulate the sarcoendoplasmic reticulum pump Ca2+ ATPase 2b and deplete endoplasmic reticulum Ca2+, leading to induction of endoplasmic reticulum stress in pancreatic beta-cells. *Diabetes* 54, 452-461

4. Wang, Q., Zhang, H., Zhao, B., and Fei, H. (2009) IL-1beta caused pancreatic beta-cells apoptosis is mediated in part by endoplasmic reticulum stress via the induction of endoplasmic reticulum Ca2+ release through the c-Jun N-terminal kinase pathway. *Mol. Cell Biochem.* 324, 183-190

5. D'Hertog, W., Overbergh, L., Lage, K., Ferreira, G. B., Maris, M., Gysemans, C., Flamez, D., Cardozo, A. K., Van den, B. G., Schoofs, L., Arckens, L., Moreau, Y., Hansen, D. A., Eizirik, D. L., Waelkens, E., and Mathieu, C. (2007) Proteomics analysis of cytokine-induced dysfunction and death in insulin-producing INS-1E cells: new insights into the pathways involved. *Mol. Cell Proteomics.* 6, 2180-2199

6. Merglen, A., Theander, S., Rubi, B., Chaffard, G., Wollheim, C. B., and Maechler, P. (2004) Glucose sensitivity and metabolism-secretion coupling studied during two-year continuous culture in INS-1E insulinoma cells. *Endocrinology* 145, 667-678

7. Pirot, P., Eizirik, D. L., and Cardozo, A. K. (2006) Interferon-gamma potentiates endoplasmic reticulum stress-induced death by reducing pancreatic beta cell defence mechanisms. *Diabetologia* 49, 1229-1236

8. Gysemans, C. A., Waer, M., Valckx, D., Laureys, J. M., Mihkalsky, D., Bouillon, R., and Mathieu, C. (2000) Early graft failure of xenogeneic islets in NOD mice is accompanied by high levels of interleukin-1 and low levels of transforming growth factor-beta mRNA in the grafts. *Diabetes* 49, 1992-1997

9. Overbergh, L., Giulietti, A., Valckx, D., Decallonne, R., Bouillon, R., and Mathieu, C. (2003) The use of real-time reverse transcriptase PCR for the quantification of cytokine gene expression. *J. Biomol. Tech.* 14, 33-43

10. Rozen, S., and Skaletsky, H. (2000) Primer3 on the WWW for general users and for biologist programmers. *Methods Mol. Biol.* 132, 365-386

11. Pfaffl, M. W. (2001) A new mathematical model for relative quantification in real-time RT-PCR. *Nucleic Acids Res.* 29, e45

12. Hinsby, A. M., Kiemer, L., Karlberg, E. O., Lage, K., Fausboll, A., Juncker, A. S., Andersen, J. S., Mann, M., and Brunak, S. (2006) A wiring of the human nucleolus. *Mol. Cell* 22, 285-295

13. Lage, K., Karlberg, E. O., Storling, Z. M., Olason, P. I., Pedersen, A. G., Rigina, O., Hinsby, A. M., Tumer, Z., Pociot, F., Tommerup, N., Moreau, Y., and Brunak, S. (2007) A human phenome-interactome network of protein complexes implicated in genetic disorders. *Nat. Biotechnol.* 25, 309-316

14. Pirot, P., Ortis, F., Cnop, M., Ma, Y., Hendershot, L. M., Eizirik, D. L., and Cardozo, A. K. (2007) Transcriptional regulation of the endoplasmic reticulum stress gene chop in pancreatic insulin-producing cells. *Diabetes* 56, 1069-1077

15. Knoblach, B., Keller, B. O., Groenendyk, J., Aldred, S., Zheng, J., Lemire, B. D., Li, L., and Michalak, M. (2003) ERp19 and ERp46, new members of the thioredoxin family of endoplasmic reticulum proteins. *Mol. Cell Proteomics.* 2, 1104-1119

16. Pirot, P., Naamane, N., Libert, F., Magnusson, N. E., Orntoft, T. F., Cardozo, A. K., and Eizirik, D. L. (2007) Global profiling of genes modified by endoplasmic reticulum stress in pancreatic beta cells reveals the early degradation of insulin mRNAs. *Diabetologia* 50, 1006-1014

17. Cnop, M., Igoillo-Esteve, M., Cunha, D. A., Ladriere, L., and Eizirik, D. L. (2008) An update on lipotoxic endoplasmic reticulum stress in pancreatic beta-cells. *Biochem. Soc. Trans.* 36, 909-915

18. Cunha, D. A., Hekerman, P., Ladriere, L., Bazarra-Castro, A., Ortis, F., Wakeham, M. C., Moore, F., Rasschaert, J., Cardozo, A. K., Bellomo, E., Overbergh, L., Mathieu, C., Lupi, R., Hai, T., Herchuelz, A., Marchetti, P., Rutter, G. A., Eizirik, D. L., and Cnop, M. (2008) Initiation and execution of lipotoxic ER stress in pancreatic beta-cells. *J. Cell Sci.* 121, 2308-2318

19. Brunner, Y., Schvartz, D., Priego-Capote, F., Coute, Y., and Sanchez, J. C. (2009) Glucotoxicity and pancreatic proteomics. *J. Proteomics.* 71, 576-591

20. Kim, I., Xu, W., and Reed, J. C. (2008) Cell death and endoplasmic reticulum stress: disease relevance and therapeutic opportunities. *Nat. Rev. Drug Discov.* 7, 1013-1030

21. Rutkowski, D. T., Arnold, S. M., Miller, C. N., Wu, J., Li, J., Gunnison, K. M., Mori, K., Sadighi Akha, A. A., Raden, D., and Kaufman, R. J. (2006) Adaptation to ER stress is mediated by differential stabilities of pro-survival and pro-apoptotic mRNAs and proteins. *PLoS. Biol.* 4, e374

22. Bomsztyk, K., Denisenko, O., and Ostrowski, J. (2004) hnRNP K: one protein multiple processes. *Bioessays* 26, 629-638

23. Mikula, M., Dzwonek, A., Karczmarski, J., Rubel, T., Dadlez, M., Wyrwicz, L. S., Bomsztyk, K., and Ostrowski, J. (2006) Landscape of the hnRNP K protein-protein interactome. *Proteomics.* 6, 2395-2406

24. Fred, R. G., and Welsh, N. (2009) The importance of RNA binding proteins in preproinsulin mRNA stability. *Mol. Cell Endocrinol.* 297, 28-33

25. Fred, R. G., Adams, C. M., and Welsh, N. (2007) Affinity binding analysis shows that hnRNP K and hnRNP E, in cytosolic extracts from human islets, binds specifically to the stabilizing segment of insulin mRNA. *Diabetologia* 50, S 207

26. Laslop, A., Becker, A., Lindberg, I., and Fischer-Colbrie, R. (2002) Proteolytic processing of chromogranins is modified in brains of transgenic mice. *Ann. N. Y. Acad. Sci.* 971, 49-52

27. Schmid, G. M., Meda, P., Caille, D., Wargent, E., O'Dowd, J., Hochstrasser, D. F., Cawthorne, M. A., and Sanchez, J. C. (2007) Inhibition of insulin secretion by betagranin, an N-terminal chromogranin A fragment. *J. Biol. Chem.* 282, 12717-12724

28. Karlsson, E., Stridsberg, M., and Sandler, S. (2000) Chromogranin-B regulation of IAPP and insulin secretion. *Regul. Pept.* 87, 33-39

29. Ledford, B. E., and Leno, G. H. (1994) ADP-ribosylation of the molecular chaperone GRP78/BiP. *Mol. Cell Biochem.* 138, 141-148

30. Freiden, P. J., Gaut, J. R., and Hendershot, L. M. (1992) Interconversion of three differentially modified and assembled forms of BiP. *EMBO J.* 11, 63-70

31. Hendershot, L. M. (2004) The ER function BiP is a master regulator of ER function. *Mt. Sinai J. Med.* 71, 289-297

32. Morrison, D. K. (2009) The 14-3-3 proteins: integrators of diverse signaling cues that impact cell fate and cancer development. *Trends Cell Biol.* 19, 16-23

33. Datta, S. R., Katsov, A., Hu, L., Petros, A., Fesik, S. W., Yaffe, M. B., and Greenberg, M. E. (2000) 14-3-3 proteins and survival kinases cooperate to inactivate BAD by BH3 domain phosphorylation. *Mol. Cell* 6, 41-51

34. Masters, S. C., Yang, H., Datta, S. R., Greenberg, M. E., and Fu, H. (2001) 14-3-3 inhibits Bad-induced cell death through interaction with serine-136. *Mol. Pharmacol.* 60, 1325-1331

35. Goldman, E. H., Chen, L., and Fu, H. (2004) Activation of apoptosis signal-regulating kinase 1 by reactive oxygen species through dephosphorylation at serine 967 and 14-3-3 dissociation. *J. Biol. Chem.* 279, 10442-10449

36. Rosenquist, M. (2003) 14-3-3 proteins in apoptosis. *Braz. J. Med. Biol. Res.* 36, 403-408

37. Masters, S. C., and Fu, H. (2001) 14-3-3 proteins mediate an essential anti-apoptotic signal. *J. Biol. Chem.* 276, 45193-45200

38. Zha, J., Harada, H., Yang, E., Jockel, J., and Korsmeyer, S. J. (1996) Serine phosphorylation of death agonist BAD in response to survival factor results in binding to 14-3-3 not BCL-X(L). *Cell* 87, 619-628

39. Yang, E., Zha, J., Jockel, J., Boise, L. H., Thompson, C. B., and Korsmeyer, S. J. (1995) Bad, a heterodimeric partner for Bcl-XL and Bcl-2, displaces Bax and promotes cell death. *Cell* 80, 285-291

40. Jiang, P., Du, W., and Wu, M. (2007) p53 and Bad: remote strangers become close friends. *Cell Res.* 17, 283-285

41. Akerfeldt, M. C., Howes, J., Chan, J. Y., Stevens, V. A., Boubenna, N., McGuire, H. M., King, C., Biden, T. J., and Laybutt, D. R. (2008) Cytokine-induced beta-cell death is independent of endoplasmic reticulum stress signaling. *Diabetes* 57, 3034-3044

Figure legends

Figure 1a: *Percentage of apoptosis induction in INS-1E cells upon exposure to a concentration range from 3.1 till 25µM CPA. Error bars indicate SEM of 3 independent experiments; * p<0.05 ** p<0.01 versus control.*

Figure 1b: *Relative mRNA expression levels of CHOP in INS-1E cells upon treatment with a concentration range from 3.1 till 25µM CPA. CHOP mRNA was quantified by Q-RT-PCR and normalized to the housekeeping gene HPRT. The mean +/- SEM of 4 independent experiments is shown * p<0.05 ** p<0.01 versus control.*

Figure 2*: CHOP western blot. Black bars show the results for the control condition, white bars for INS-1E cells treated with 25µM CPA. CHOP levels increased from 0.034±0.009 to 0.298±0.088 at 6h and from 0.033±0.008 to 0.243±0.029 at 12h. Error bars indicate SEM of 3 independent experiments; * p<0.05 ** p<0.01.*

Figure 3*: Relative mRNA expression levels of A) HSPA5, B) HYOU1 and C) PDIA6 normalized for HPRT. Rectangular markers (□) indicate control and circular markers (○) indicate CPA treated INS-1E cells. Error bars indicate SEM of 3 experiments; * p<0.05 ** p<0.01 versus control.*

Figure 4*: Relative mRNA expression levels of A) prohormone convertase 2 and B) insulin 2. INS-1E cells were exposed to 25µM CPA. mRNA was quantified by Q-RT-PCR and normalized to the housekeeping gene HPRT. Severe ER stress caused a decrease in mRNA levels of both insulin and PCSK2. Rectangular markers (□) indicate control and circular markers (○) indicate CPA treated INS-1E cells. Error bars indicate SEM of 3 independent experiments; * p<0.05 ** p<0.01 versus control.*

Figure 5: *Insulin secretion of INS-1E cells, treated with 25µM CPA for 6, 12 and 24h. Insulin release was measured upon stimulation with 20mM glucose. Black bars show the results for the control condition, white bars for INS-1E cells treated with 25µM CPA. Error bars indicate SEM of 3 independent experiments; ** p<0.01 versus control.*

Figure 6: *Overview of glycolysis and Krebs cycle pathways with enzymes identified as being differential expressed upon exposure of INS-1E cells with 6.25µM CPA for a) 6h and b) 12h. The identified enzymes are depicted in bold next to the reaction they effect. Up-or downregulation of the enzymes is depicted with block arrows.*

Figure 7: *Relative mRNA expression levels of HSPA5 upon treatment of INS-1E cells with 6.25µM CPA. mRNA was quantified by Q-RT-PCR and normalized to the housekeeping gene HPRT. Rectangular markers (□) indicate control and circular markers (○) indicate CPA treated INS-1E cells. Error bars indicate SEM of 3 experiments; ** p<0.01*

Figure 8*: Insulin release after treatment of INS-1E cells with 6.25µM CPA for 6, 12 and 24h. Insulin release was measured upon stimulation with 20mM glucose. Black bars show the results for the control condition, white bars for INS-1E cells treated with 6.25µM CPA. Error bars indicate SEM of 3 independent experiments; * p<0.05*

Supplemental figure 1*: Representative images of the different spot maps of INS-1E cells exposed to either 6.25µM CPA or 25µM CPA in two different pH ranges. In yellow are the spot boundaries of the differential expressed spots, with the according spot numbers.*

Supplemental figure 2: *Network analysis of the identified differential expressed proteins after a) 6h of exposure to 25µM CPA (p<1e-6) and b) 12h of exposure to 25µM CPA(p<1e-6). Colored circles represent proteins that were identified in this study, and grey circles represent interconnecting proteins revealed by the network software program. A maximum of two interconnecting proteins is allowed. The identified proteins were colored according to their function: proteins involved in metabolism, blue; protein synthesis/modification, light pink; ionic channels and related proteins, light blue; processing of peptides, dark pink; cell adhesion and cytoskeleton, dark green; RNA synthesis/turnover, yellow; cell cycle, brown; defense/repair mechanisms, orange; calcium binding, light green; and miscellaneous, purple.*

Supplemental figure 3: *Network analysis of the identified differential expressed proteins after a) 6h of exposure to 6.25µM CPA and b) 12h of exposure to 6.25µM CPA and c) 24h of exposure to 6.25µM CPA (all p<5e-6). Colored circles represent proteins that were identified in this study, and grey circles represent interconnecting proteins revealed by the network software program. A maximum of two interconnecting proteins is allowed. The identified proteins were colored according to their function: proteins involved in metabolism, blue; protein synthesis/modification, light pink; ionic channels and related proteins, light blue; processing of peptides, dark pink; cell adhesion and cytoskeleton, dark green; RNA synthesis/turnover, yellow; cell cycle, brown; defense/repair mechanisms, orange; calcium binding, light green; and miscellaneous, purple.*

Figure 1a

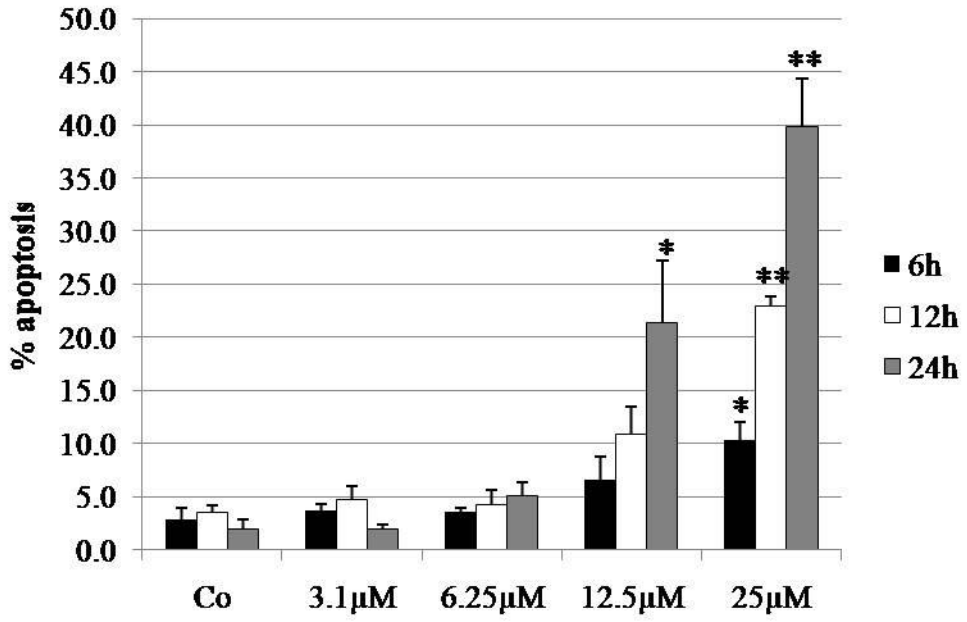


Figure 1b:

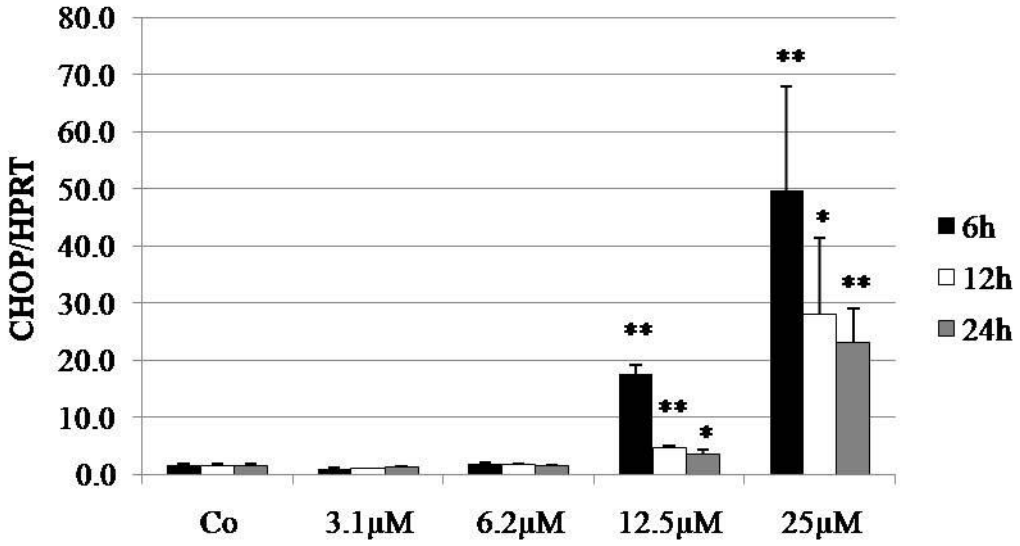


Figure 2:

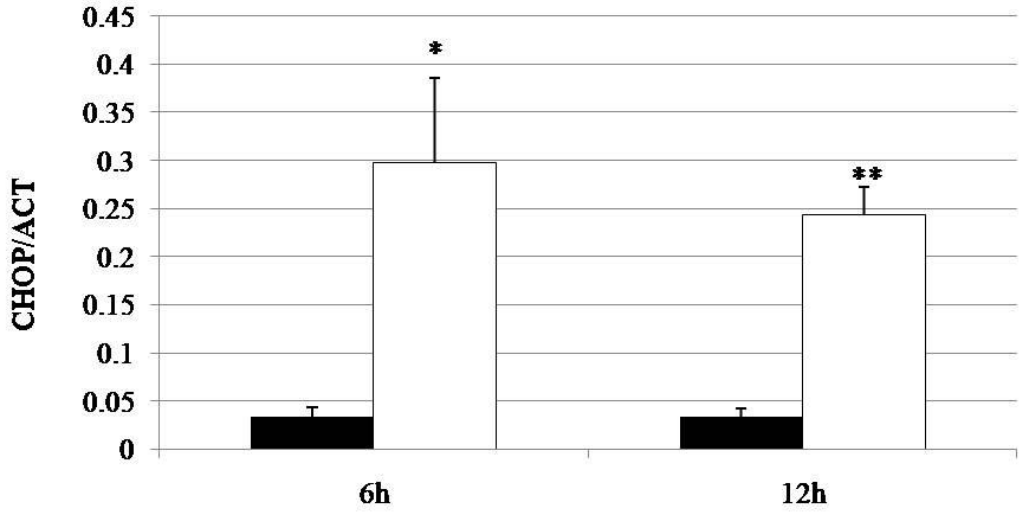


Figure 3a:

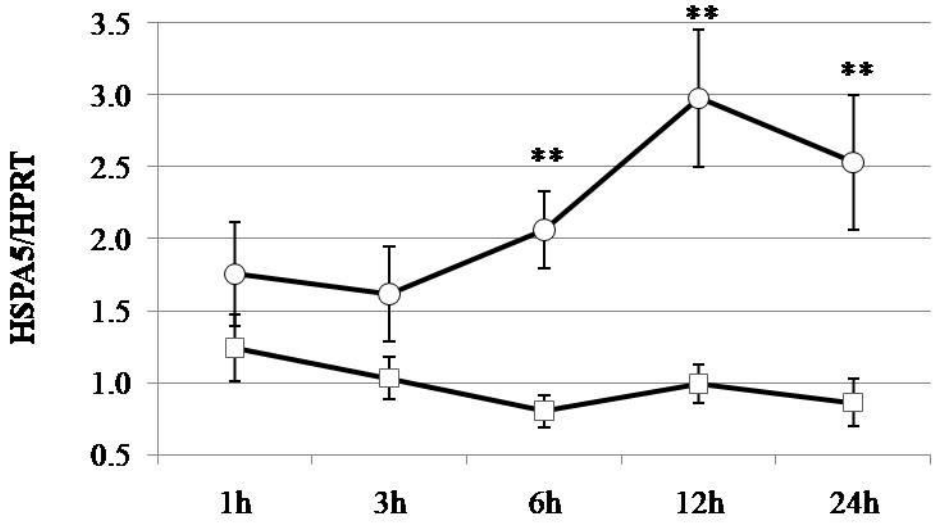


Figure 3b:

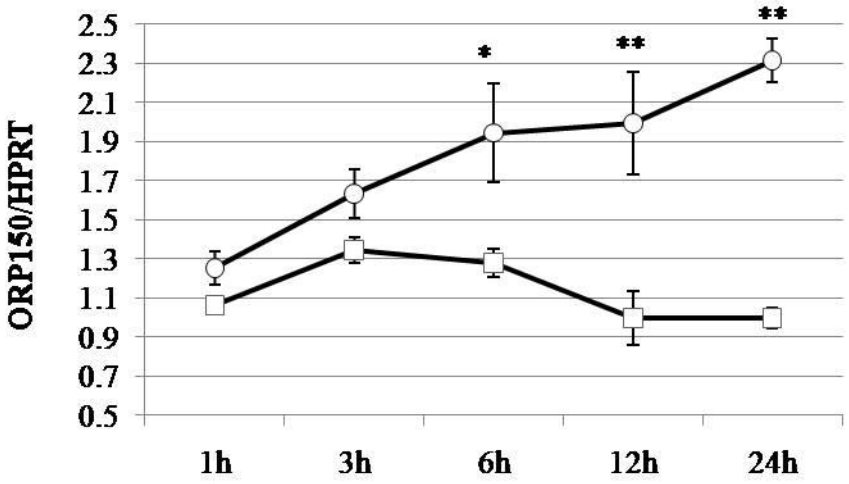


Figure 3c:

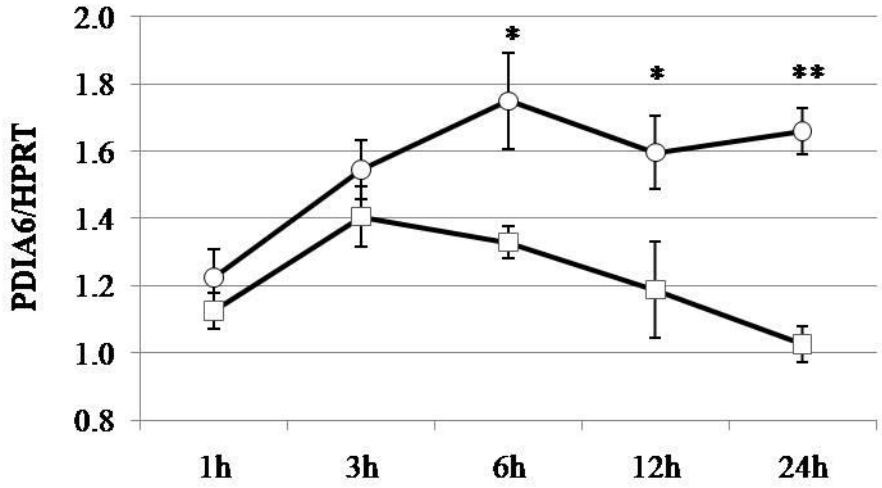


Figure 4a:

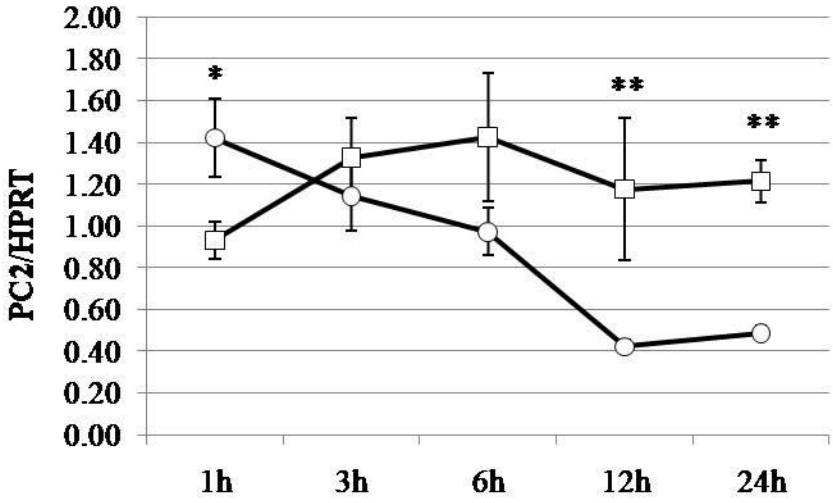


Figure 4b:

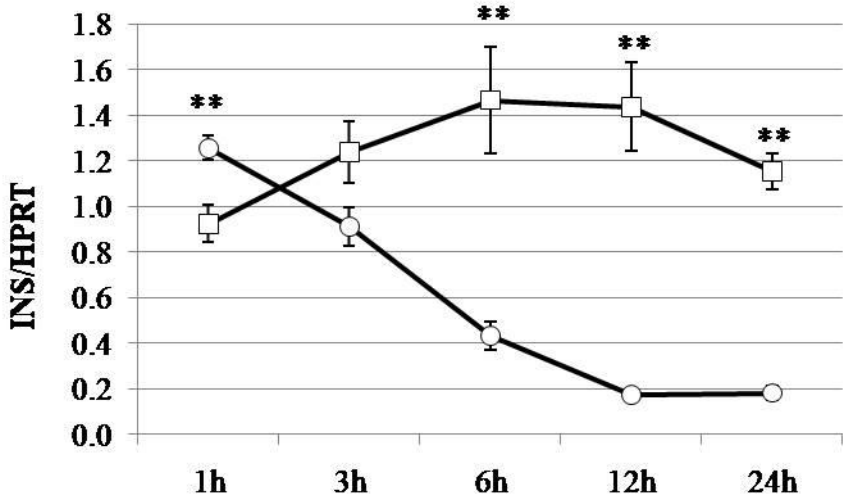


Figure 5:

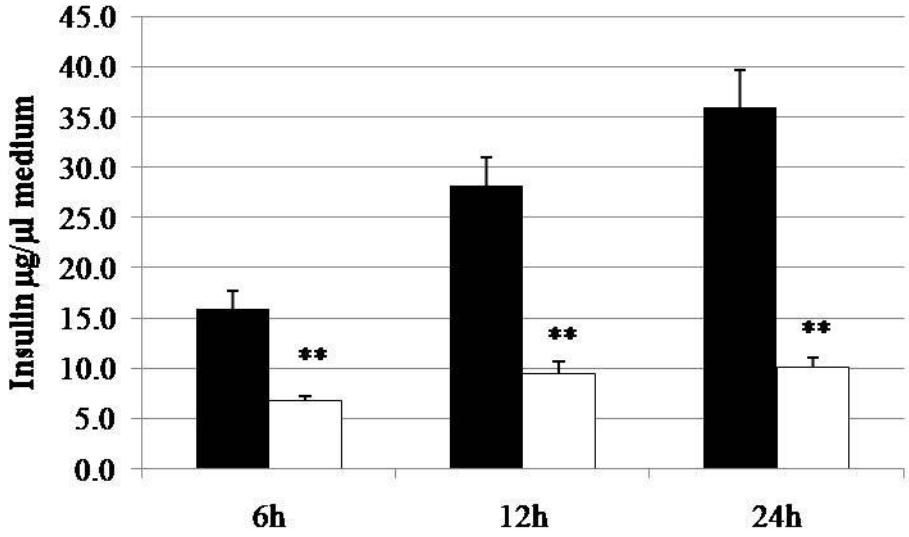


Figure 6a:

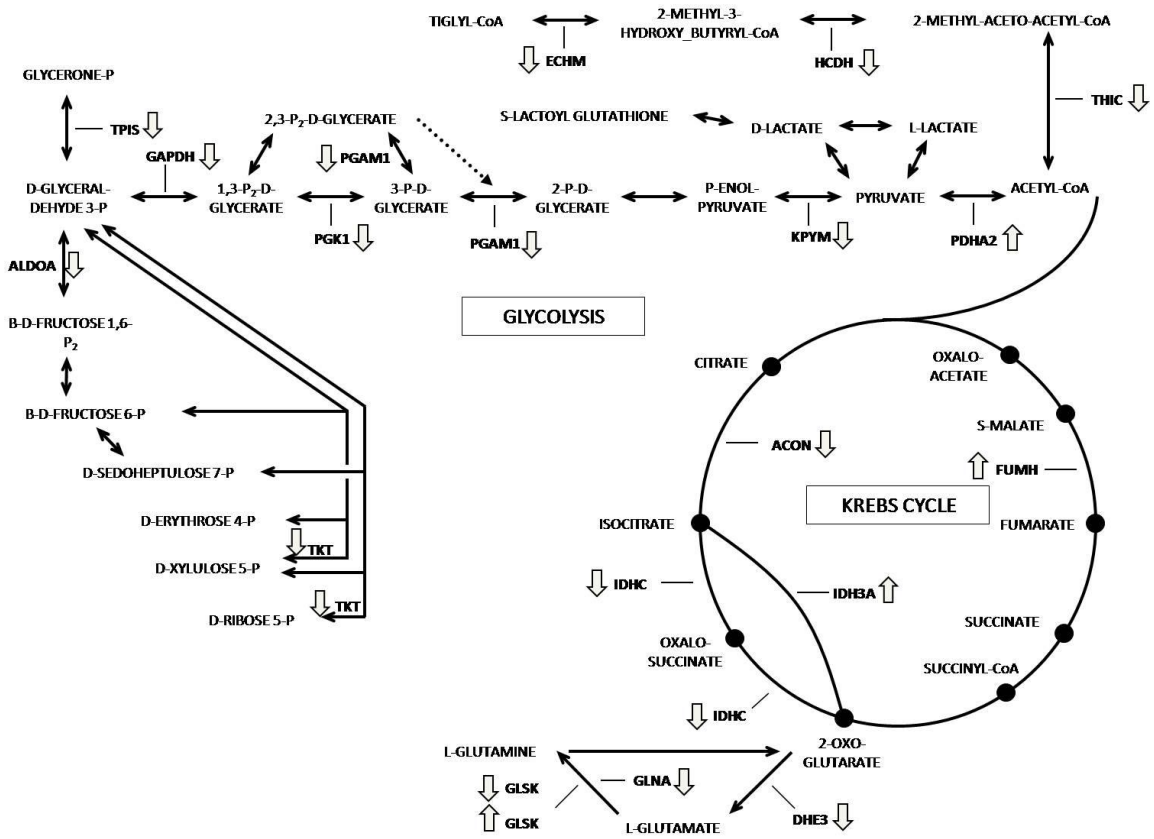

TIGLYL-CoA
ECHM
2-METHYL-3-HYDROXY_BUTYRYL-CoA
HCDH
2-METHYL-ACETO-ACETYL-CoA
THIC
GLYCERONE-P
TPIS
2,3-P2-D-GLYCERATE
S-LACTOYL GLUTATHIONE
D-LACTATE
L-LACTATE
GAPDH
PGAM1
D-GLYCERAL-DEHYDE 3-P
1,3-P2-D-GLYCERATE
3-P-D-GLYCERATE
2-P-D-GLYCERATE
P-ENOL-PYRUVATE
PYRUVATE
ACETYL-CoA
PGK1
PGAM1
KPYM
PDHA2
ALDOA
GLYCOLYSIS
B-D-FRUCTOSE 1,6-P2
B-D-FRUCTOSE 6-P
D-SEDOHEPTULOSE 7-P
D-ERYTHROSE 4-P
TKT
D-XYLULOSE 5-P
TKT
D-RIBOSE 5-P
CITRATE
OXALO-ACETATE
S-MALATE
ACON
FUMH
KREBS CYCLE
ISOCITRATE
FUMARATE
IDHC
IDH3A
SUCCINATE
OXALO-SUCCINATE
SUCCINYL-CoA
IDHC
L-GLUTAMINE
2-OXO-GLUTARATE
GLSK
GLNA
GLSK
L-GLUTAMATE
DHE3

Figure 6b:

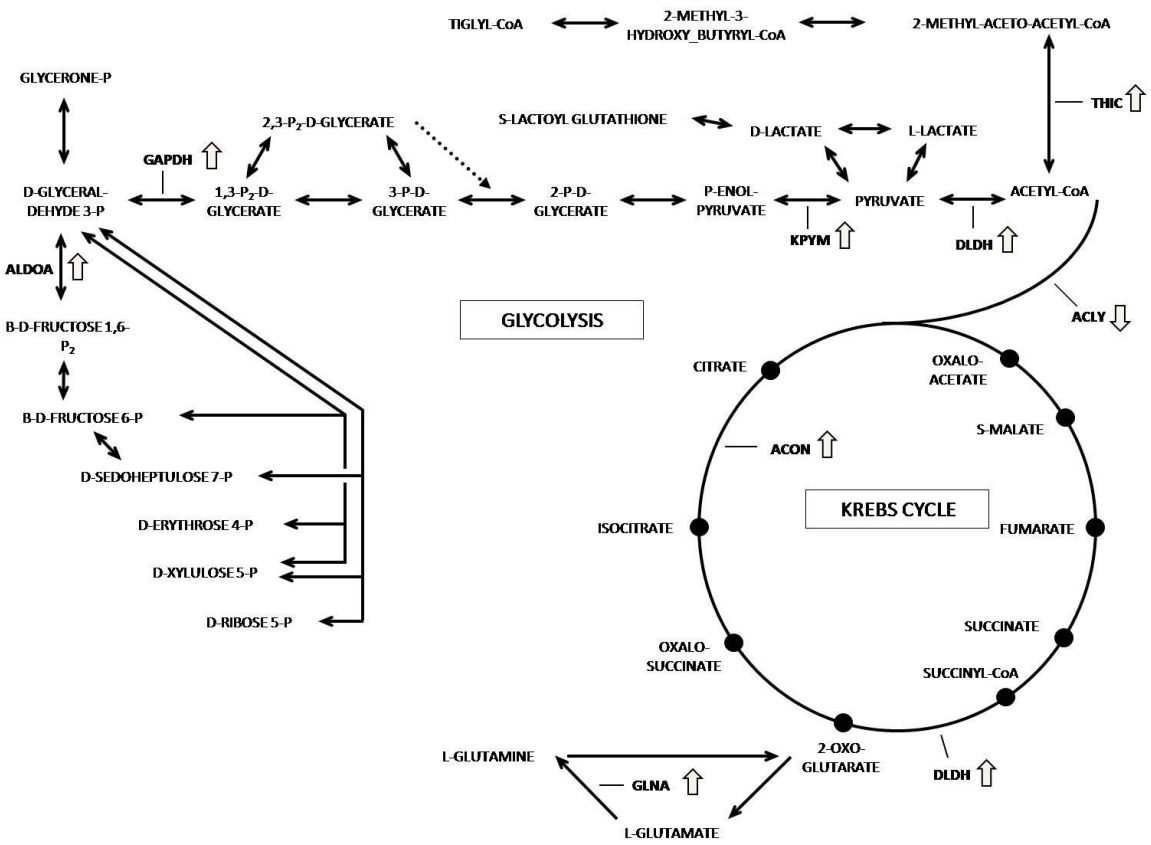


Figure 7:

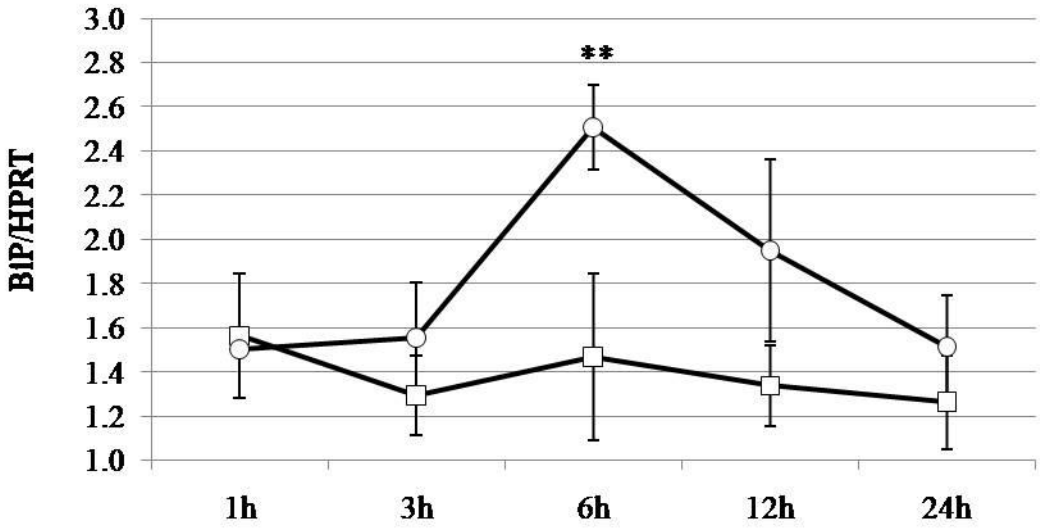
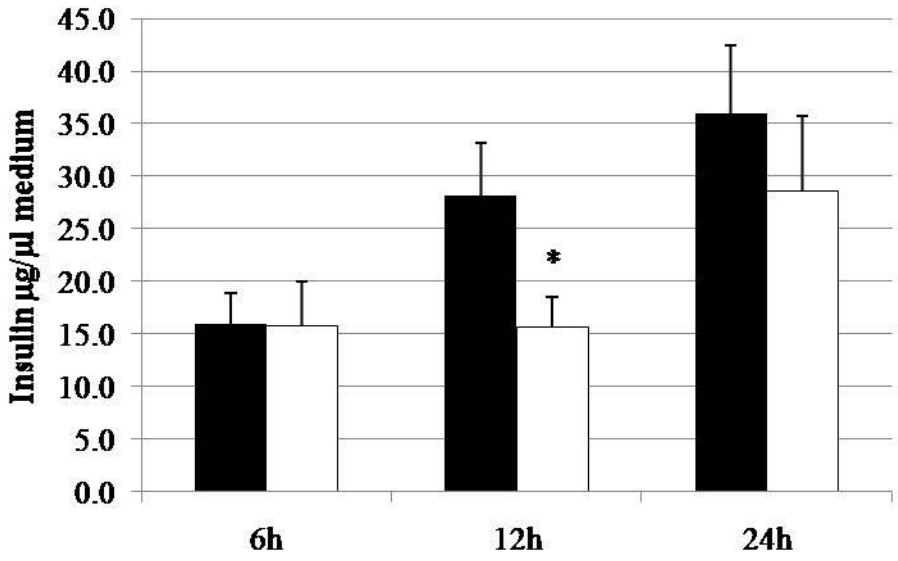
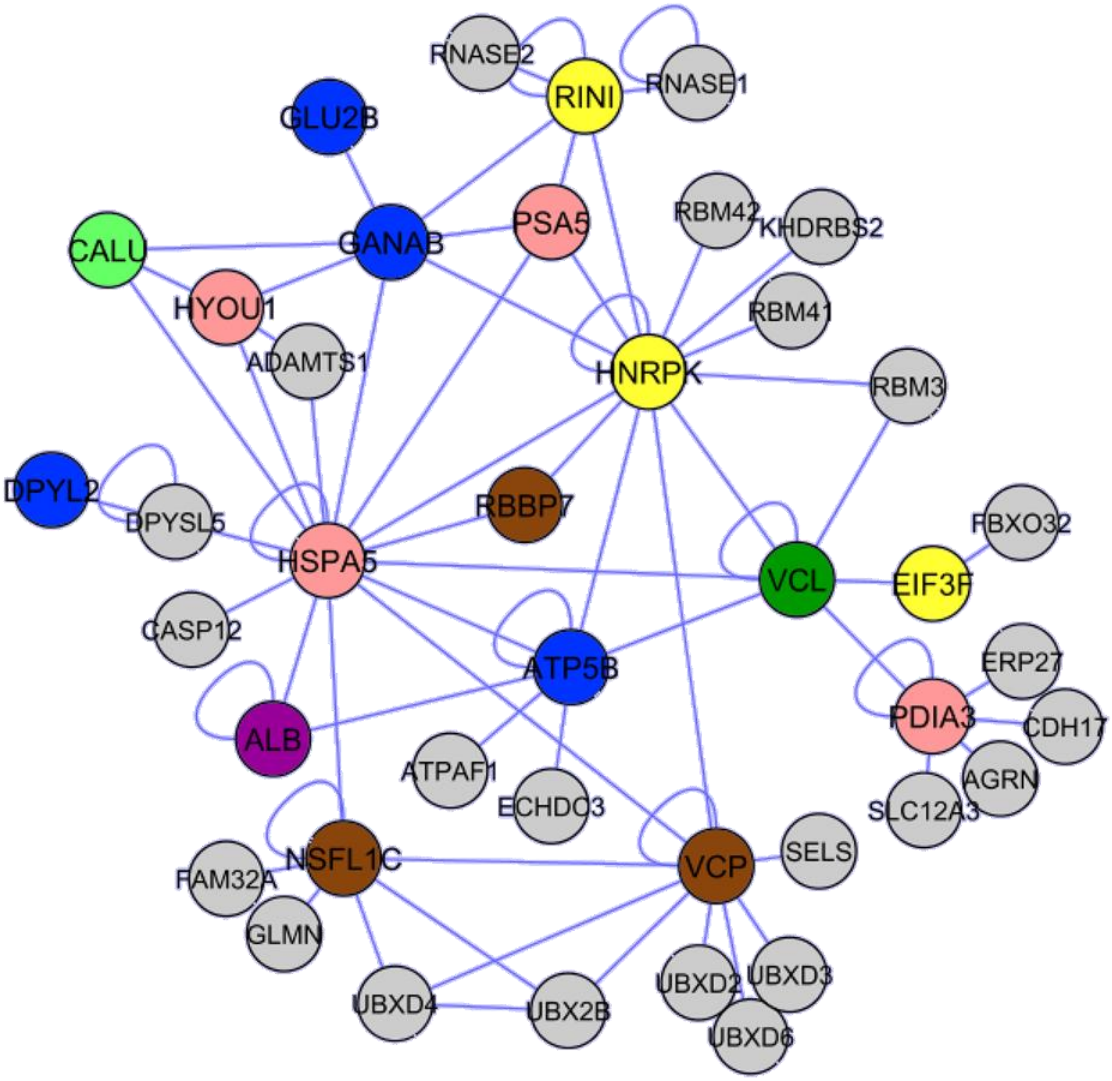


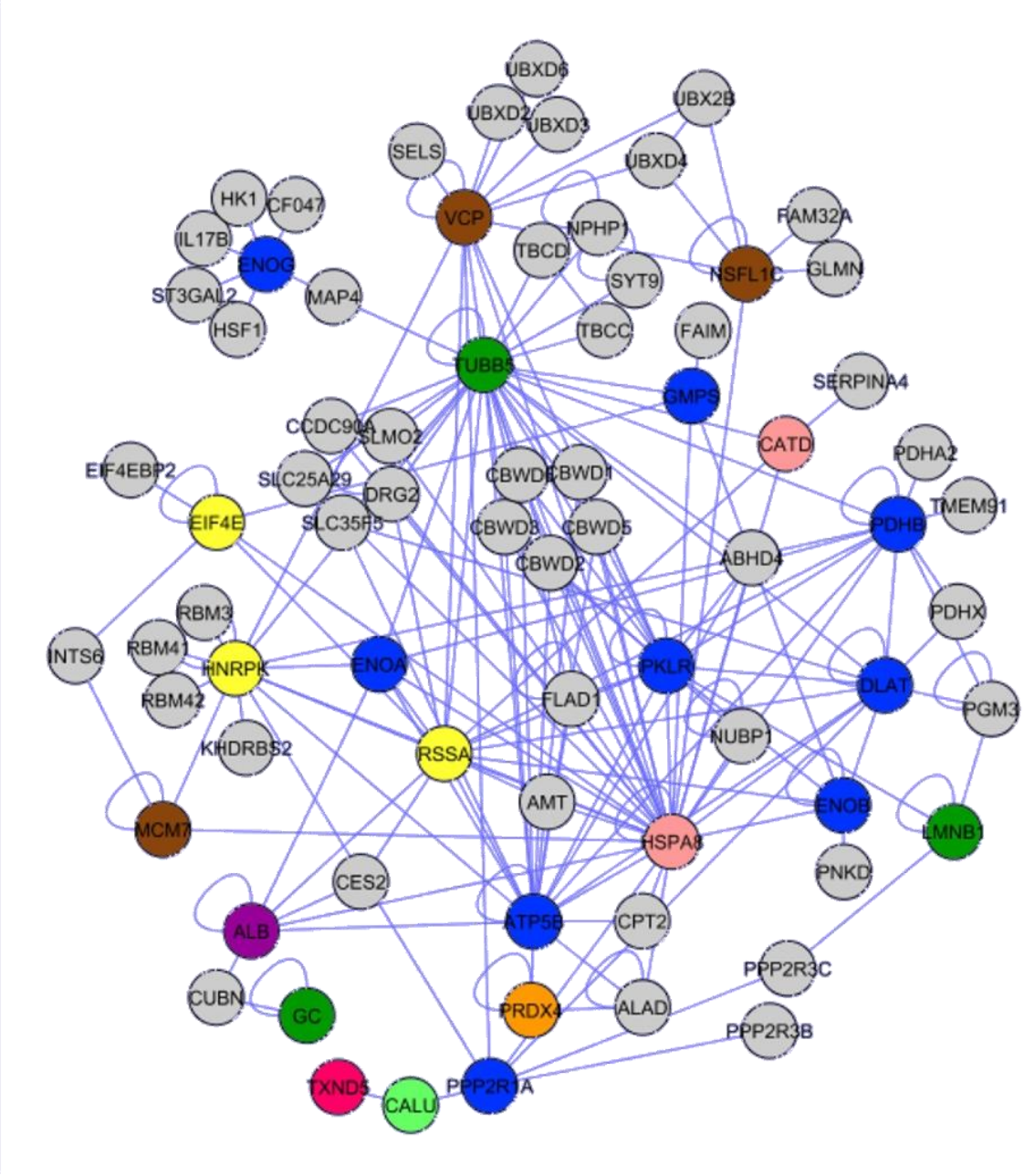
Figure 8:



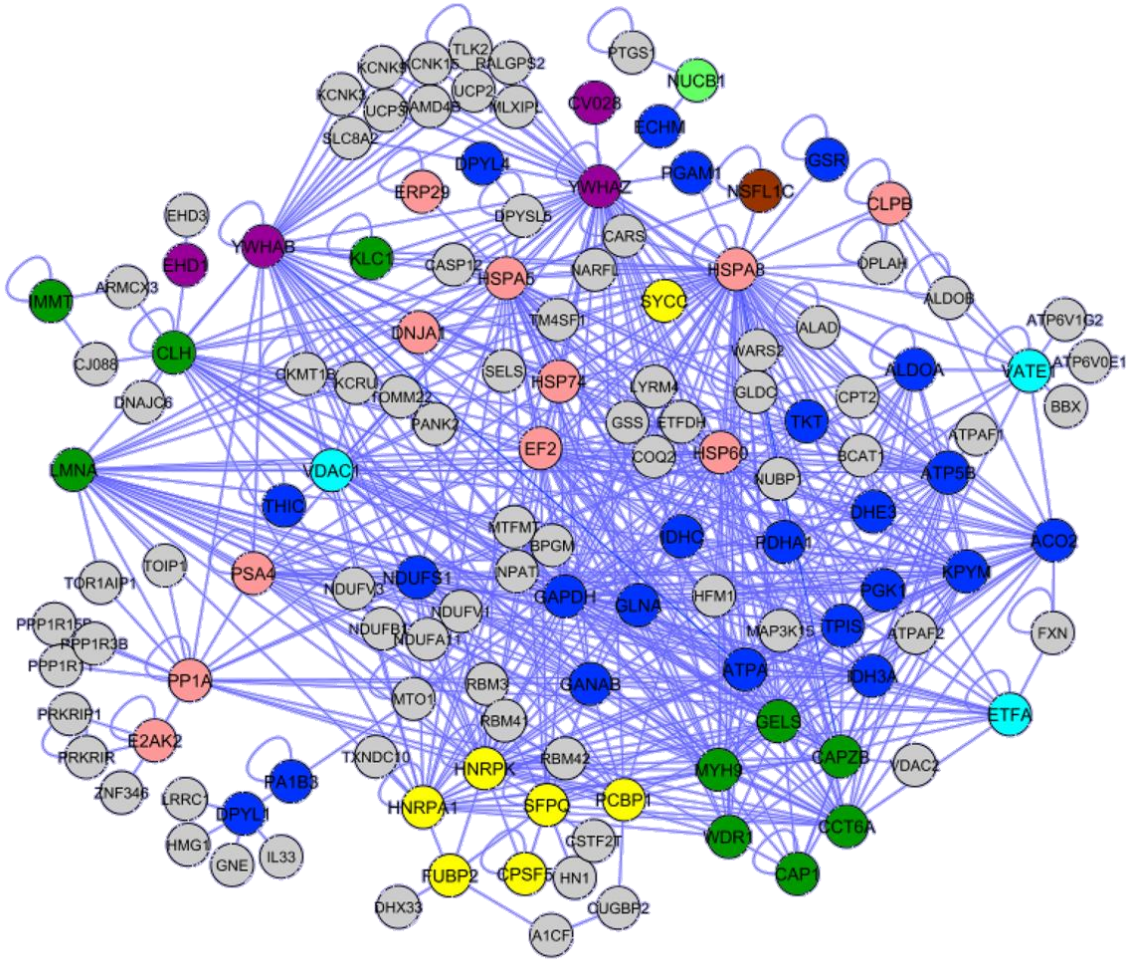
Supplemental figure 2a:



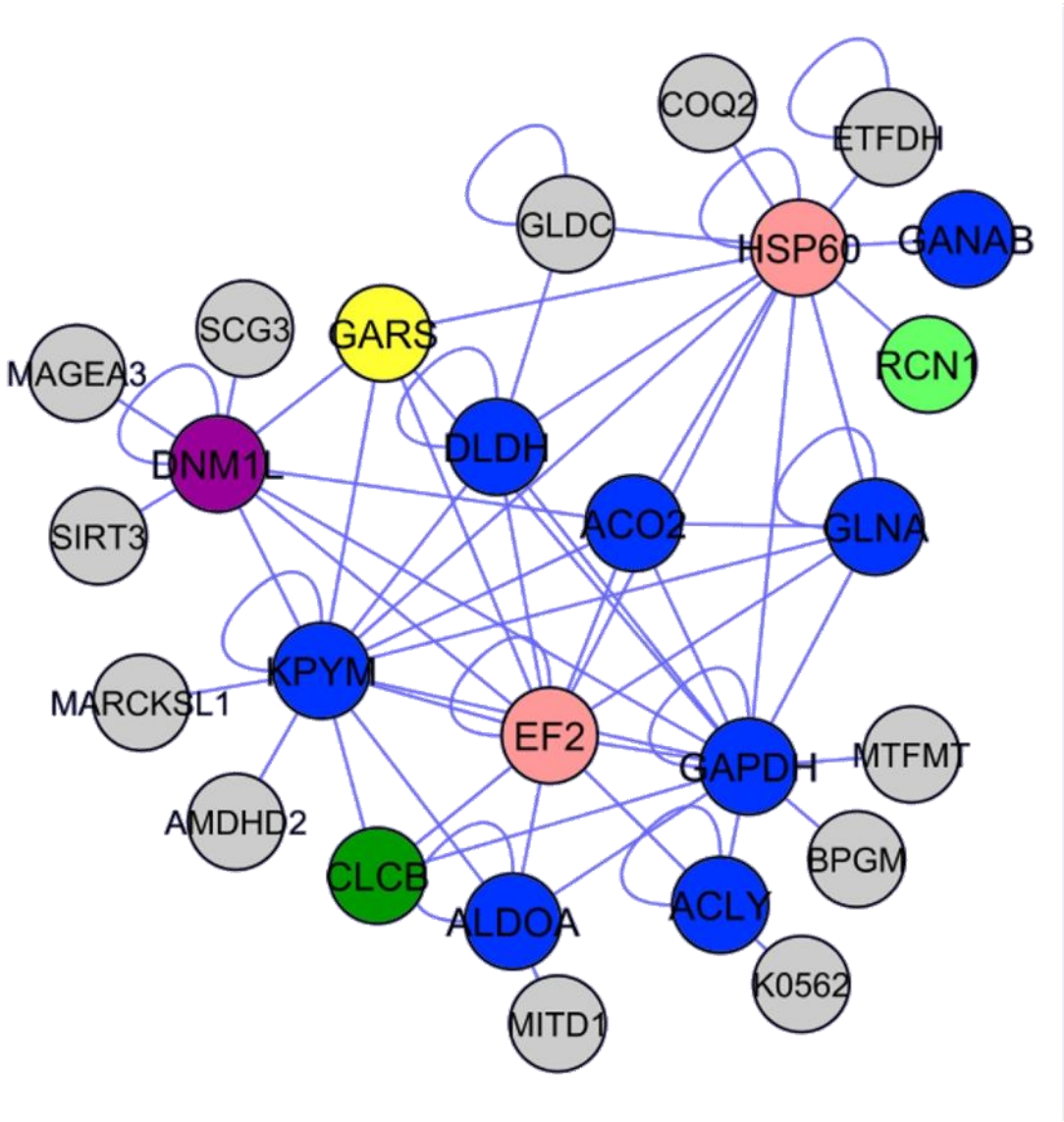
Supplemental figure 2b:



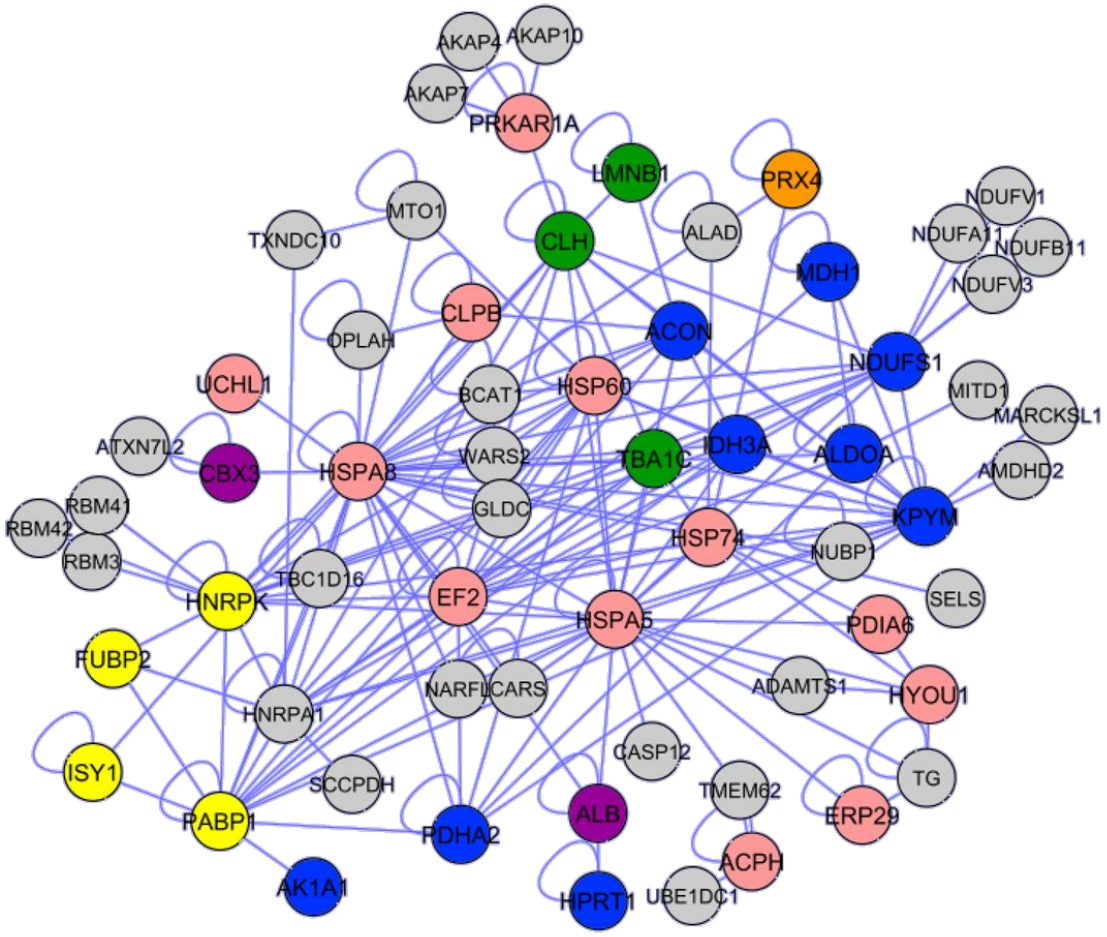
Supplemental figure 3a:



Supplemental figure 3b:



Supplemental figure 3c:


AKAP4
AKAP10
AKAP7
PRKAR1A
LMNB1
PRX4
NDUFV1
MTO1
TXNDC10
CLH
ALAD
NDUFA11
NDUFB11
MDH1
NDUFV3
CLPB
ACON
DPLAH
NDUFS1
UCHL1
BCAT1
HSP60
MITD1
MARCKSL1
ATXN7L2
CBX3
HSPA8
WARS2
TBA1C
IDH3A
ALDOA
AMDHD2
RBM41
RBM42
GLDC
KPYM
HSP74
RBM3
NUBP1
TBC1D16
HNRPK
EF2
SELS
HSPA5
PDIA6
FUBP2
NARFL
CARS
ADAMTS1
HYOU1
HNRPA1
CASP12
ISY1
SCCPDH
TMEM62
TG
ALB
ERP29
PABP1
PDHA2
ACPH
AK1A1
HPRT1
UBE1DC1